Solubility and Mechanism of Dissolution of Dihydrated and Anhydrous Uric Acid

Edoardo Mentasti*

Istituto di Chimica Analitica, Università di Torino, 10125 Torino, Italy

Caterina Rinaudo

Istituto di Mineralogia, Cristallografia e Geochimica, Università di Torino, 10123 Torino, Italy

Roland Boistelle

Centre de Recherche sur les Mécanismes de la Croissance Cristalline, CNRS, Campus de Luminy, Case 913, 13288 Marseille Cedex 9, France

The solubilities of dihydrated orthorhombic and anhydrous monoclinic forms of uric acid (UA) have been investigated spectrophotometrically at different temperatures (2.6–50.0 °C). Data have also been collected for the different solubilities as a function of pH and have been assigned to the different species of uric acid in protolytic equilibrium at the investigated conditions. The kinetics of uric acid dissolution into aqueous media have also been investigated under different experimental conditions and the results have been interpreted in order to characterize the mechanisms involved in the dissolution step as well as in the reverse process. Equilibrium thermodynamic quantities have been derived and their values have been discussed with reference to the proposed mechanisms.

Introduction

According to the growth conditions, uric acid (UA) can crystallize in two forms, either anhydrous ($C_5H_4N_4O_3$) or hydrated ($C_5H_4N_4O_3 \cdot 2H_2O$). The former modification is monoclinic, whereas the latter orthorhombic (*1–5*). The crystallization of both phases was investigated as a function of temperature, pH, and uric acid concentration (*6*). The occurrence of the dihydrated crystals is promoted by low temperatures or low pHs as well as by high solute concentration. However, these crystals are always unstable and transform into anhydrous ones (*7–9*). This phase transition, which occurs also in aqueous solution, is due to the difference in solubility and thermodynamic stability of the two crystalline species (*7*). A few papers have been reported in the literature on the solubility of uric acid in either aqueous (*9*) or buffered (*10*, *11*) solutions. On the other hand, the phase equilibria between the different solid forms of this compound of relevant biological interest have been generally disregarded.

The availability of the equilibrium quotient for the first proton-release step from UA at different temperatures, as well as the possibility of keeping both orthorhombic as well as monoclinic forms of the acid for relatively long times, enables the independent study of the solubility in water of undissociated and dissociated monoanion forms of both uric acid modifications. Uric acid is an important component of urinary stones (*3–5*, *8*), so that information on the solubility of this compound is also of great interest.

In connection with these implications, it seemed helpful to investigate the mechanism which drives the solution process. To this purpose, some measurements of the dissolution rate were carried out. These experiments were performed with crystals of the anhydrous modification, which is the only thermodynamically stable form. The dissolution has been investigated at different acidities (buffered medium between pH 6.50 and 4.50, and pure water) and at different quantities of excess uric acid. This was done in order to shed light on the mechanisms and reaction order of both dissolution and reverse processes and to clarify the role of surface processes and/or diffusion processes between the crystal–solution interface and the water of the bulk. The temperature was kept constant between 2.6 and 50.0 °C and the dissociation constant of the first proton of uric acid ($H_2U \rightleftarrows HU^- + H^+$) (*9*) was obtained by interpolating earlier data for each investigated temperature (*9*).

Experimental Section

Crystals. Uric Acid (E. Merck or C. Erba) was recrystallized several times from aqueous solutions before it was used. In order to measure the dissolution rate, it was necessary to grow large amounts of crystals of the anhydrous modification. To this purpose, aqueous solutions were saturated at about 90 °C and left to crystallize at room temperature overnight. This method leads to a mixture of both modifications. In order to eliminate the hydrated crystals, we separated the precipitate from the solution by filtration and stored the precipitate for 1 week in a desiccator under vacuum and in the presence of phosphorous pentoxide. This time was sufficient to achieve the phase transition. The crystals were then sieved in order to get a uniform distribution ranging from 0.1 to 0.2 mm.

For the solubility determinations it was necessary to grow the two modifications separately. Aqueous solutions were saturated at about 60 °C with the recrystallized material prepared as above. They were then left to cool to 20 and 37 °C, temperatures at which the hydrated and anhydrous modifications grew, respectively (*6*). After 2 or 3 days the crystal size was about 0.5 mm.

Doubly distilled water was used throughout.

Solutions. For the solubility determinations only pure water has been used as a medium. For the kinetic measurements, buffered solutions were also used. They were prepared by mixing $KH_2PO_4 + Na_2HPO_4$ or $CH_3COOH + CH_3COONa$ solutions in the appropriate ratios in order to get pH 6.00, 5.50 or 5.00, 4.50, respectively (*12*).

Procedure. The rate of dissolution of anhydrous uric acid was followed by mixing, with constant stirring, weighed amounts of UA with 100 mL of water or buffered solution, previously thermostated at 37.0 °C. UA portions were in large excess with respect to the dissolved quantities ($C_{UA,tot} \gg [UA]_{sol}$) at attained equilibrium so that the solid could be assumed as constant during each experiment. After the dissolution was started, portions of the solution were withdrawn with manual suction by means of a filtering syringe built from a glass cylin-

0021-9568/83/1728-0247$01.50/0

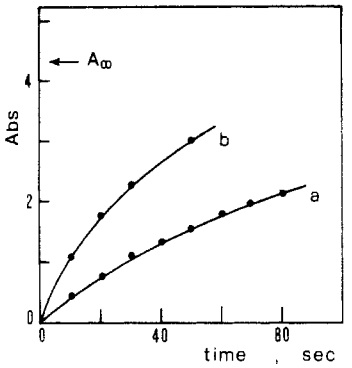

Figure 1. Variation of absorbance at 285 nm for the dissolution of 25 (a) and 100 (b) mg of anhydrous UA in 100 mL of pure water as function of time at 37.0 °C.

der, a rubber piston (derived from a disposable hypodermic syringe), and a glass-frit disk (pore size 15–40 μm glued with epoxy resin to the bottom of the glass cylinder).

The manual filtering operation allowed us to withdraw about 1 mL of solution in less than 1 s. The use of a series of syringes enabled us to obtain five to six portions of the solution at different times; then, after appropriate dilution, the dissolved uric acid concentration was measured spectrophotometrically.

Solubility measurements have been performed on equilibrated solutions between bidistilled water (absence of buffers and salts, i.e., null ionic strength added) and hydrated or anhydrous UA in excess with respect to the saturation. In the case of the hydrated form, the attained equilibrium (ca. 10 min after mixing the solid with thermostated water at 25 °C) is transient since later the dihydrate slowly transforms into the anhydrous modification with a decrease of solubility. The solubility measurements were mainly made by means of a spectrophotometer. In the case of the anhydrous phase, some additional measurements were carried out by using a method already described elsewhere (*13*). The temperature of saturation is determined by alternatively raising and lowering the temperature and observing the appearance and dissappearance of the crystals.

In order to calibrate the spectrophotometer, we have taken UV spectra (Cary 219, Varian, Palo Alto, CA) from UA solutions of constant concentration and at different pH values between 4.00 and 7.00.

The solution absorbance depends on the concentration according to the relation

$$A = \epsilon b [\mathrm{UA}]_{\mathrm{tot}} \qquad (1)$$

where ϵ is the molar absorptivity (L mol^{-1} cm^{-1}), b is the spectrophotometer cell thickness (b = 1.00 cm in our case), and $[\mathrm{UA}]_{\mathrm{tot}}$ is the concentration of dissolved uric acid (mol L^{-1}). A maximum of absorption at 280 nm (at the lower pHs) is present, which is then shifted to 290 nm (at higher pHs), in agreement with the data reported by Finlayson and Smith (*14*) owing to the equilibrium set up between the undissociated form (H_2U) and the conjugated base (HU^-) of uric acid. An isosbestic point is present at 285 nm and therefore this wavelength has been adopted in order to monitor the total dissolved UA concentration at every acidity. A series of undersaturated UA solutions were prepared from weighed portions in order to obtain the molar absorptivity at the isosbestic point, which was found to be $\epsilon_{UA}(285)$ = 11950 L mol^{-1} cm^{-1}, in agreement with the data reported earlier (*14*).

Results and Discussion

Kinetics of Dissolution. As can be seen from Figure 1, which is a typical dissolution plot, the dissolution follows an exponential monotonical variation with time showing a decrease of rate with the decreasing of the actual undersaturation of the solution as a function of time. The undersaturation, which is defined as [undersat] = $[\mathrm{UA}]_\infty - [\mathrm{UA}]_t$ (where $[\mathrm{UA}]_\infty$ and $[\mathrm{UA}]_t$ are the concentrations of uric acid in the saturated solution and at time t, respectively), is proportional to $A_\infty - A_t$, where A_∞ and A_t represent the absorbance at equilibrium and at time t after addition of the solid to the water.

Table I. First-Order Observed Rate Constants, k_{obsd} (s^{-1}), at 37.0 °C[a] for the Dissolution of Different Amounts of Anhydrous Uric Acid as a Function of Acidity

	mg of UA in 100 mL of soln			
	25	50	75	100
pure water	0.009	0.016	0.018	0.025
pH 6.00	0.008	0.018	0.020	0.028
5.50	0.007	0.011	0.019	0.027
5.00	0.008	0.011	0.021	0.025
4.50	0.008	0.011	0.020	0.025

[a] See eq 5.

Plots of $-\ln (A_\infty - A_t)$ as a function of time were found to be linear, thus showing that the rate of dissolution is proportional to the first power of the undersaturation, i.e., is of first order with respect to the undersaturation. In fact, for the reaction

$$\mathrm{UA}_{\mathrm{solid}} \xrightarrow{k_{obsd}} \mathrm{UA}_{\mathrm{solution}} \qquad (2)$$

(where k_{obsd} is the observed dissolution rate constant) the rate of dissolution is given by

$$\frac{d[\mathrm{UA}]_{sol}}{dt} = -\frac{dC_{\mathrm{UA,solid}}}{dt} = -\frac{d[\mathrm{undersat}]}{dt} = k_{obsd}[\mathrm{undersat}]$$
$$= k_{obsd}([\mathrm{UA}]_\infty - [\mathrm{UA}]_t) = k_{obsd}(A_\infty - A_t)/\epsilon b \qquad (3)$$

from which it follows that

$$-\frac{d(A_\infty - A_t)}{(A_\infty - A_t)} = k_{obsd}\, dt \qquad (4)$$

and, after integration

$$\ln [A_\infty/(A_\infty - A_t)] = k_{obsd}t \qquad (5)$$

The experimental data conform with eq 5 and, from the slopes of plots of $-\ln (A_\infty - A_t)$ vs. time, the observed dissolution rate constants k_{obsd} could be evaluated.

The rate at which saturation is attained is governed by the two opposite processes

$$\text{solid uric acid} \underset{\text{(b) reverse rate}}{\overset{\text{(a) forward rate}}{\rightleftharpoons}} \text{dissolved uric acid} \qquad (6a,b)$$

In the investigated conditions the dissolution step (a) proceeds at constant rate since the solid UA is in large excess with respect to the dissolved quantity at any time. Since the observed dissolution rate is the difference between the rates of the two processes in eq 6 and since step 6a has a constant rate, the observed first-order behavior must be ascribed to step 6b. At the earlier stages of the dissolution process the dissolved UA concentration is very low, and therefore step 6b is almost absent and the dissolution rate is mainly governed by the rate of step 6a; at longer times the rate of reaction 6b increases according to the lowered undersaturation and the overall process is therefore slowed down. The rate of dissolution thus becomes zero when the rate of reaction 6b becomes equal to the rate of step 6a, i.e., when saturation condition is gained.

Table I collects the observed rate constants obtained at the investigated pH values. At every acidity, measurements have been performed with different uric acid quantities. The observed rate constants showed a linear dependence on the total UA added. Therefore, the following expression can be written:

$$k_{obsd} = \bar{k} C_{UA} \qquad (7)$$

Table II. Experimental Solubilities ($[UA]_{tot}$) of Uric Acid Forms at Different Temperatures, Obtained Spectrophotometrically, and Computation of Equilibrium Concentration of the Species Involved in the Saturated Dihydrated and Anhydrous Uric Acid Solution for Different Experimental Conditions[a]

	$10^4[UA]_{tot}$, M			$10^5[H^+]$,[c] M		f[d]		$10^4[H_2U]$,[e] M		$10^5[HU^-]$, M	
T, °C	dihyd	anhyd	pK_{1A}[b]	dihyd	anhyd	dihyd	anhyd	dihyd	anhyd	dihyd	anhyd
2.6	0.962	0.711	5.79	1.17	0.99	1.13	1.16	0.85	0.61	1.17	1.00
9.3	1.42	1.05	5.71	1.56	1.33	1.12	1.15	1.26	0.92	1.57	1.34
25.0	3.39	2.07	5.53	3.00	2.31	1.10	1.12	3.09	1.83	3.02	2.33
37.0	6.56	3.66	5.42	4.80	3.54	1.07	1.11	6.07	3.31	4.85	3.56
50.0	14.40	6.28	5.29	8.33	5.41	1.06	1.08	13.56	5.73	8.36	5.46

[a] The reported values represent the mean of replicated values. Uncertainty on duplicates was always better than 4%. [b] Interpolated from the data reported in ref 9. [c] Computed, after iteration, from eq 10. [d] $f = 1 + K_{1A}/[H^+]$. [e] Computed from eq 13.

(where C_{UA} represents the weight in grams of added solid uric acid) and the following values for $\bar{k} = k_{obsd}/C_{UA}$ were obtained at 37.0 °C: $\bar{k}$ (s^{-1} g^{-1}) = 0.28 at pH 6.00; $\bar{k}$ = 0.25 at pH 5.50; $\bar{k}$ = 0.25 at pH 5.00; $\bar{k}$ = 0.25 at pH 4.50; and $\bar{k}$ = 0.27 in pure water. The increase of the quantity of solid UA added has no effect on the rate of step b of eq 6 or on the solubility, since the reverse step (b) is independent of the excess solid UA; therefore, its effect is displayed by reaction 6a, which will become faster with increasing quantity of UA, i.e., with increasing the solid–solution interface. If the linear dependence of eq 7 must therefore be ascribed to step 6a, then also the forward dissolution process proceeds with a first-order dependence on the quantity of solid UA, in other words, on the surface of the solid UA.

Turning now to the effect of acidity, the data reported above show that the specific rate constants $\bar{k}$ are independent of acidity. At increasing pH, the solubility of UA is greatly enhanced. Also, the uric acid quantity dissolved in the unit time increases with increasing pH but the relative variation of the undersaturation, which represents the rate of dissolution, is independent of acidity. In other words, if a variation from pH_1 to pH_2 doubles the solubility of UA, the time needed in order to gain, e.g., 50% saturation is the same for the two pHs irrespective of the double quantity dissolved at pH_2 compared to pH_1.

The meaning of the reported observed (or specific) rate constants is therefore related to the time ($t_{1/2}$) in which a relative undersaturation 0.50 is reached, i.e., the time in which the dissolved UA gives a concentration $^1/_2$ with respect to the saturated solution.

$$t_{1/2} = (\ln 2)/k_{obsd} \qquad t_{1/2}^* = (\ln 2)/\bar{k} \tag{8}$$

where $t_{1/2}$ refers to a solid UA quantity corresponding to the "observed" condition, whereas $t_{1/2}^*$ refers to 1 g of UA. In conclusion, the mechanism of dissolution proceeds through a fairly fast composite process with first-order dependence on both forward and reverse dissolution pathways.

The effect of acidity on the rate of dissolution is absent even if a very strong dependence on the solubility of UA is observed. These data and the derived considerations do not allow us to clearly assess whether the dissolution process is governed by interfacial or diffusive steps.

A first-order dependence on UA quantity would be expected in the case of interfacial mechanisms. In the case of a diffusion-controlled process a leveling of the rate, as a function of UA, would be expected. Either of these mechanisms could be operative in the observed system; in fact, also in the second case a lowering of the reaction order with increasing UA could not be investigated since higher quantities would have given dissolutions too fast to be followed with our procedure. In the case of a diffusion-limited mechanism the nature of the diffusing species in the layer between solid UA and solution "in bulk" should be greatly affected by variations of acidity, in particular at pH values around the pK_{1A} value of uric acid: small pH changes would change the form of the predominant species of uric acid in solution, greatly affecting the rate of dissolution. The absence of this effect, therefore, seems to suggest a surface-controlled mechanism as operative.

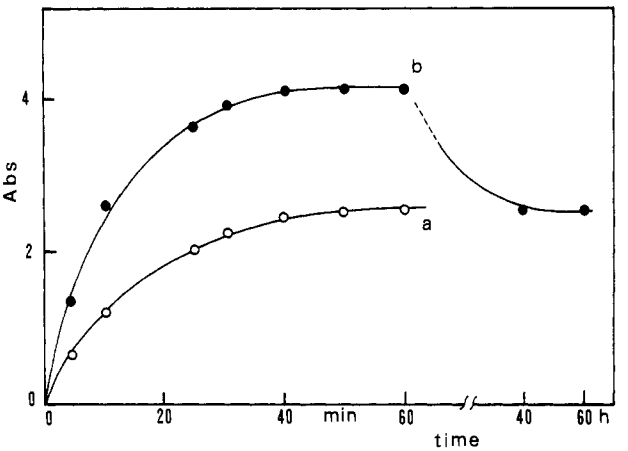

Figure 2. Variation of absorbance at 285 nm as a function of time for the dissolution of anhydrous (a) and dihydrated (b) UA (for details see the section on solubility).

Solubility. Figure 2 shows typical curves for the dissolution process involving either the dihydrated or the anhydrous phase when dissolution is determined spectrophotometrically. In both cases 50 mg of dihydrated or anhydrous UA crystals was added to 50 mL of water thermostated at 25.0 °C. The absorbance increases rapidly with time up to a maximum, the value of which depends on the investigated phase. The time necessary to reach the plateau depends on crystal size, temperature, and amounts of solid UA added to the water. If 50 mg of UA is added to 50 mL of water, the maxima are reached after 30 min at 25.0 °C but only after 2 h at 9.3 °C. In addition, the maximum remains stable only for the anhydrous modification, decreasing rapidly when the dihydrate is concerned until the plateau of the anhydrous modification is reached (see Figure 2). Dissolution in water has been measured spectrophotometrically at 2.6, 9.3, 25.0, 37.0, and 50.0 °C (±0.1 °C).

The total concentrations $[UA]_{tot}$ or uric acid dissolved at every temperature have been calculated with eq 1. The results for both dihydrated and anhydrous forms are collected in Table II, from which it turns out that the solubilities are nearly the same at low temperatures, whereas at 37.0 °C the solubility of the dihydrate is about twice the solubility of the anhydrous phase.

An usual plot of ln $[UA]_{tot}$ vs. $1/T$ (Figure 3) enables the calculation of the enthalpy (ΔH_d) and entropy (ΔS_d) of dissolution for the two crystalline species, taking into account the conversion of M units into mole fractions. For the anhydrous phase ΔH_d = 8.1 ± 0.1 kcal mol^{-1} and ΔS_d = 2.3 ± 0.3 eu. For the dihydrate ΔH_d = 10.0 ± 0.1 kcal mol^{-1} and ΔS_d = 9.7 ± 0.3 eu. From the solubility data and from the equilibrium constant obtained by interpolation of the pK_{1A} values (9) vs. $1/T$, it was possible to calculate the pH values of the solutions

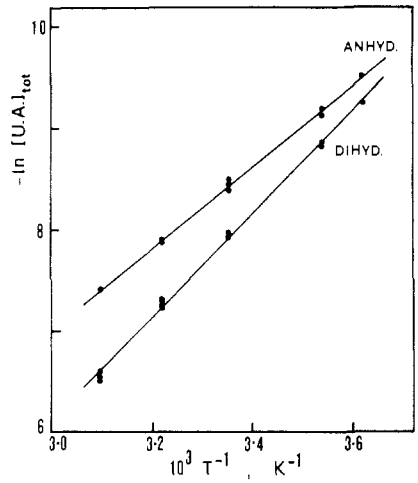

Figure 3. Plots of total dissolved UA equilibrated with solid anhydrous and dihydrated UA as a function of reciprocal absolute temperature.

saturated at different temperatures. As a matter of fact, we have

$$[UA]_{tot} = [H_2U] + [HU^-] \quad (9)$$

where the terms H_2U and HU^- represent the undissociated and dissociated portions of uric acid in solution. In addition

$$[H^+] = [HU^-] = \{K_{1A}([UA]_{tot} - [H^+])\}^{1/2} \quad (10)$$

where

$$K_{1A} = [H^+][HU^-]/[H_2U] \quad (11)$$

The results are collected in Table II. From eq 10 and 11 we get

$$[UA]_{tot} = [H_2U](1 + 1\ K_{1A}/[H^+]) \quad (12)$$

If we call $f = 1 + K_{1A}/[H^+]$, it obviously results that

$$[H_2U] = [UA]_{tot}/f \quad (13)$$

$$[H^+] = [UA]_{tot}\,(1 - 1/f) \quad (14)$$

From the calculated data (Table II) it is now possible to know the solubility of both modifications at different temperatures and pH values. Figure 4 shows the solubility curves at 25.0 and 37.0 °C for pH values ranging from 4.00 to 5.00.

Finally, in Figure 5 we have plotted not only the $[UA]_{tot}$ values measured spectrophotometrically vs. $1/T$ (curves A and B) but also the solubility values concerning the anhydrous phase which has been determined by the method of temperature fluctuations (*13*) (curve C). The difference between curves B and C is probably due to the presence of a small quantity of dihydrated crystals in the case of curve C. The enthalpy and entropy of dissolution calculated from these last data are $\Delta H_d = 7.8 \pm 0.1$ kcal mol^{-1} and $\Delta S_d = 1.7 \pm 0.3$ eu, values fairly close to those obtained with the spectrophotometric method.

Turning to the mechanism, since the solubility increases with increasing pH and also the dissociation $H_2U \rightleftarrows HU^- + H^+$ is shifted to the right, H_2U species will be less soluble than HU^-, so that saturated uric acid solutions will be saturated with respect to the undissociated uric acid only.

The solvation of the undissociated dissolved uric acid is low due to the structure of the molecule. Since saturation and therefore solubility are governed by this species, mechanisms of structuring and destructuring of the solvent around the solid as it goes into solution seem to be low (H_2U species is noncharged and its structure does not show markedly polar centers). Moreover, the interactions between the molecules in the solid are of the hydrogen-bonded dipolar type; therefore, high ΔH values are not expected for the breakage of the interactions in the solid and the solvent–solute interaction formation during

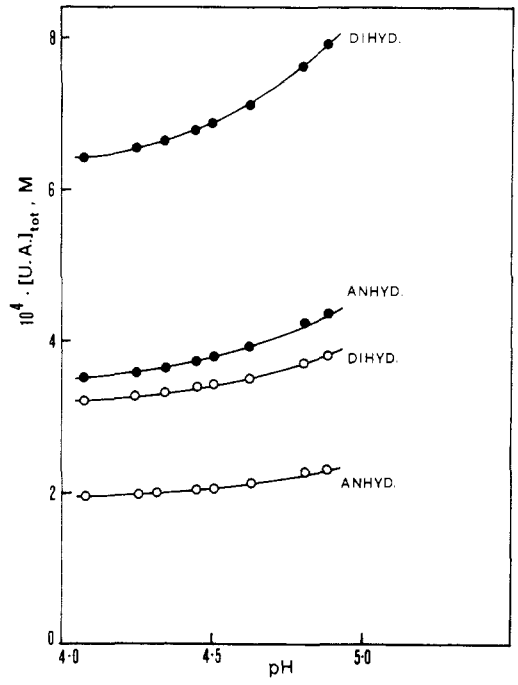

Figure 4. Solubility curves for dihydrated and anhydrous UA as a function of pH (open circles, 25.0 °C; closed circles, 37.0 °C).

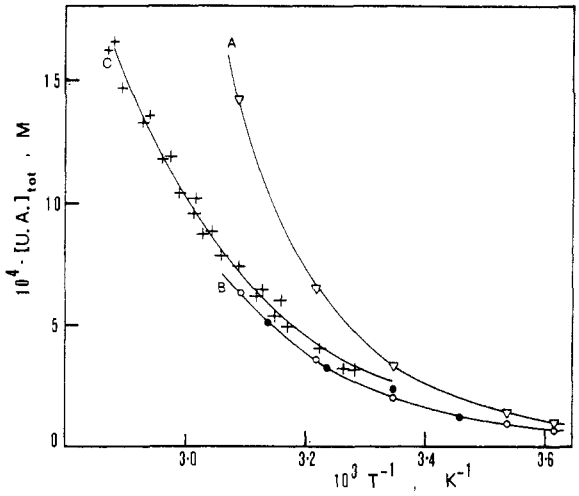

Figure 5. Solubility curves as a function of reciprocal absolute temperature for dihydrated orthorhombic (A) and anhydrous monoclinic (B) UA (the closed points, included with our results, are taken from ref *9*). Curve C is obtained for the anhydrous form with the temperature fluctuation method (*13*) (for details see the text).

dissolution. This composite mechanism should not contribute to a decrease of entropy (low structuring of the solvent) in respect to normal dissolution of the solid, as it has been found experimentally.

Conclusion

Spectrophotometric measurements on the dynamics of the dissolution of anhydrous UA crystals enabled us to ascertain the reaction order with respect to the solid UA. The described method does not allow us to distinguish unambiguously between a diffusion-limited and a surfacial process, even if some considerations, derived from the acidity effects, lead us to prefer the latter.

The solubility data were obtained for the anhydrous and dihydrated crystals as a function of pH, temperature, and UA concentration and compared with previous results (*6*, *7*).

The present data point out also that, at physiological conditions of temperature and acidity, the dihydrated form is much

more soluble (see Figure 4) than the anhydrous one; also, its solubility/pH slope is much more pronounced. This last feature comes out, in part, from the lowering of the pK_{1A} value at increasing temperatures. Therefore, the higher occurrence in human stones (*3-5*, *8*) of the anhydrous crystals can be a consequence not only of their thermodynamic stability but also of the higher solubility of the hydrated ones. On the contrary, the nonpolar structure of UA, as well as the thermodynamic parameter values, clearly shows that a very minor role is played by solute-solvent interactions.

Registry No. Uric acid, 69-93-2.

Literature Cited

(1) Ringertz, H. *Acta Crystallogr.* **1965**, *19*, 286.
(2) Ringertz, H. *Acta Crystallogr.* **1966**, *20*, 397.
(3) Shirely, R. *Science* **1966**, *152*, 1512.
(4) Sutor, D. J.; Scheidt, S. *Br. J. Urol.* **1968**, *40*, 22.
(5) Lonsdale, K.; Sutor, D. J. *Sov. Phys.—Crystallogr.* (*Engl. Transl.*) **1972**, *16*, 1060.
(6) Rinaudo, C.; Boistelle, R. *J. Cryst. Growth* **1980**, *49*, 569.
(7) Boistelle, R.; Rinaudo, C. *J. Cryst. Growth* **1981**, *53*, 1.
(8) Hesse, A.; Schneider, H. J.; Berg, W.; Hienzsch, E. *Invest. Urol.* **1975**, *12*, 405.
(9) Lam, C. Y.; Nancollas, G. H.; Ko, S. *J. Invest. Urol.* **1978**, *15*, 473.
(10) Sperling, O.; Kedem, O.; De Vries, A. *Rev. Fr. Etud. Clin. Biol.* **1966**, *11*, 40.
(11) Porter, P. *Res. Vet. Sci.* **1983**, *4*, 580.
(12) Meites, L. "Handbook of Analytical Chemistry"; McGraw-Hill: New York, 1963.
(13) Lundager Madsen, H. E.; Boistelle, R. *J. Chem. Soc., Faraday Trans. 1* **1976**, *72*, 1078.
(14) Finlayson, B.; Smith, A. *J. Chem. Eng. Data* **1974**, *19*, 94.

Received for review May 4, 1982. Revised manuscript received December 6, 1982. Accepted January 21, 1983.

Density of Molten $NaAlCl_4$. A Reinvestigation

Rolf W. Berg,* Hans A. Hjuler, and Niels J. Bjerrum*

The Technical University of Denmark, Chemistry Department A, DK-2800 Lyngby, Denmark

The automated "float" method was used over a temperature range of 160–600 °C to measure liquid densities of NaCl–$AlCl_3$ mixtures containing 50 mol % $AlCl_3$. Linear and quadratic expressions in temperature were fitted to the data, which compare satisfactorily with the literature.

Introduction

Molten NaCl–$AlCl_3$ mixtures are important solvents and their densities have been often studied (*1–10*). The results of these studies are not entirely consistent. Most recently two extensive papers appeared (*5*, *7*) which seem to be quite reliable.

Fannin et al. (*5*), using dilatometric tubes, studied densities in the acidic range of the phase diagram (i.e., $AlCl_3$ mol % from 50 to 75) at low temperatures (from the melting points up to ca. 350 °C) and reported their results as a quadratic equation in temperature as well as mole fraction (nine parameters). Their results were in good agreement (within 1%) with Boston's (*4*) and Midorikawa's (*3*) older data.

Sato et al. (*7*), on the other hand, using a manometric method, studied the density of the LiCl–NaCl–$AlCl_3$ system in the basic range (i.e., less than 50 mol % $AlCl_3$) at high temperatures (from ca. 527 to ca. 927 °C). Their density data were reported as a linear function of temperature and quadratic function of composition (12 parameters).

By comparing these two equations and their ranges of validity, we see that the temperature range from ca. 350 to ca. 527 °C is excluded and both equations cover the equimolar $NaAlCl_4$ melt density only at their boundary of validity. Of more importance, quantitative calculations for $NaAlCl_4$ (see later) show that Fannin's equation (*5*) gives too low densities when extrapolated upward in temperature and that Sato's equation (*7*) gives too low densities when extrapolated downward in temperature, relative to each other. This means that the curvature of the density dependence on temperature is not properly accounted for, or it means that one or another of the two equations is not correct for the $NaAlCl_4$ melt.

The present investigation was performed in order to find a single temperature expression for the density of the equimolar NaCl–$AlCl_3$ melt and at the same time to test the validity of the equations of Fannin (*5*) and Sato (*7*).

Table I. Experimental Densities and Temperatures of $NaAlCl_4$ Melts

densities of floats, g cm^{-3}		measd temp at the indicated mole fraction, °C	
at 25 °C	at measd temp	$X_{NaCl} = 0.4999_8$[b]	$X_{NaCl} = 0.5000_2$[c]
1.709 60	1.709 14	165.6 (10)[a]	
1.681 04	1.680 51		195.4 (8)
1.653 82	1.653 20		231.6 (9)
1.641 96	1.641 30		245.3 (11)
1.625 75	1.625 05		266.4 (10)
1.600 40	1.599 62	299.8 (9)	
1.518 10	1.517 09	409.0 (10)	
1.441 07	1.439 87	511.5 (13)	
1.382 30	1.380 96	594.2 (15)	

[a] I.e., 165.6 ± 1.0 °C. [b] Scan rate = 50 °C h^{-1}. [c] Scan rate = 12 °C h^{-1}.

Experimental Section

The densities were measured by the automated float method (*11*, *12*) with a new microprocessor controlling/registering unit constructed in our laboratory. The method is based on magnetic detection of quartz floats with iron cores as they pass a differential transformer. The idea is that the temperature and hence the density of the melt (placed in a long tube together with the floats) are increased or decreased gradually. The density of the quartz floats does not change much with temperature, and, if the difference in density between floats and melt originally is small, the floats will consequently either sink or float at a given temperature. Floats of different densities were made by sealing small weights of iron (50–300 mg) into small pieces of quartz tubes (outside diameter 6 mm and length 20–30 mm). The densities at 20 °C of these floats were obtained by the Archimedian method by weighing the floats in air and in water and correcting for the buoyancy of the air.

The furnace and its regulation have been described in detail previously in connection with the introduction of the "automated float method" (*11*). Passage temperatures were detected by

0021-9568/83/1728-0251$01.50/0